Taylor & Francis
Taylor & Francis Group

REVIEW

Check for updates

Crystallography and the liquid crystal phase: a new approach to structural studies on a thermo-tropic smectic Schiff base

Oscar Enrique Piro[a], Gustavo Alberto Echeverría[a] and Fabio Daniel Cukiernik[b]

[a]Departamento de Física, Facultad de Ciencias Exactas, Universidad Nacional de La Plata and Institute IFLP (CONICET, CCT-La Plata), La Plata, Argentina; [b]INQUIMAE (Conicet-UBA) and DQIAQF, Facultad de Ciencias Exactas y Naturales, Universidad de Buenos Aires, CABA, Argentina

ABSTRACT

In spite of the apparent contradiction between 'liquid crystals' (LC, materials exhibiting some degree of disorder) and 'crystallography' (a paradigmatic ordered kingdom), X-ray diffraction (XRD) studies make a substantial contribution to the field of LC. Focusing this review on smectic (Sm, lamellar) LC, we first describe how extremely careful XRD studies performed on mono-domain samples in the LC phase helped to elucidate the molecular structure of ordered Sm phases. Then, we describe selected examples in which single-crystal (SC) XRD on the solid-state phase of the mesogens provided information about their supra-molecular organization in the Sm phase. Finally, we present a different approach to this problem in the case of a thermo-tropic Schiff base (SB) which undergoes crystal $\leftrightarrow$ LC $\leftrightarrow$ isotropic liquid phase transformations. By combined SC and variable-temperature powder XRD, we show that the SB LC is a hexatic smectic B phase that derives from the crystal phase by relatively small topological changes promoted by the set-in of thermal rotational disorder around the long SB molecular axis.

Q1

1. Introduction

Liquid crystals (LC) are a fascinating class of materials. The allure that they exert on scientists can be traced to their unique physical properties. The term 'liquid crystals' looks like an intrinsic contradiction; it was first coined in 1889 by Otto Lehmann [1] ('Flussige Kristale') to refer to materials exhibiting simultaneously some properties typical of liquids (like fluidity) and others characteristic of crystalline solids (like birefringence). The term LC is still in use to describe these materials, and actually it applies to a wide class of the more general kind called 'mesomorphic materials', 'mesogenic compounds' or 'materials exhibiting mesophases', that is, phases with partial positional and/or orientational order. LCs proved to be a well-suited 'testing-bench' for different theories on fluids [2–8]. In addition, the amazing textures observed by polarized optical microscopy (POM) provide an aesthetic pleasure to researchers in the field [9]. Most people nowadays are familiar with the acronym LC describing liquid crystals, thanks to their already widespread electro-optical applications (especially in displays) available in the market of technology products [10].

CONTACT Oscar Enrique Piro ✉ piro@fisica.unlp.edu.ar

The partial degree of orientation/positional order that characterizes LCs can be achieved either by heating a crystalline pure compound or by cooling isotropic liquids, that is, as a consequence of thermal effects (*thermo-tropic* mesophases). In addition, there exists a second class of LCs where the perturbing effect on the crystal order is due to solvent (usually water), eventually coupled to thermal effects (*lyotropic* mesophases). Although dozens of different types of mesophases arising from mesogens with very different molecular shapes are known [11], the more archetypal ones are (i) columnar mesophases (Col) based on disc-like (discotic) mesogens, (ii) nematic mesophases (N) based on either discotic or rod-like (calamitic) mesogens, (iii) poorly ordered smectic A (SmA) and smectic C (SmC) mesophases based on calamitic mesogens, and (iv) relatively ordered hexatic smectic mesophases (SmB, SmF, SmI) based on calamitic mesogens. All these mesophases are schematically depicted in Figure 1. A relevant point to both basic aspects and applications lies in the relationship between the structure of the mesophases and the anisotropy of their physical properties, such as charge migration, energy transport or refraction index (which anisotropy yields the typical birefringence used for both LC phase identification and display applications). Unless specific treatments aimed to obtain samples oriented at a macroscopic scale are performed, the described organization extends over micron-sized domains; consequently, as their optical axis orientation varies at that scale length, LC are often seen as opaque fluids, the aspect they showed when discovered by Reinitzer [12]. In turn, both the physical properties and their anisotropy are strongly dependent on the molecular structure. Most mesogens contain a central core (a relatively flat unit having high electron polarizability) and surrounding aliphatic chains connected to the core through linkers [13]. However, there exist nowadays hundreds of examples that depart from this archetypal molecular structure.

Nematic phases are the less ordered mesophases. They have also been called in the past 'orientationally ordered liquids': in an N mesophase, molecules are roughly parallel to one
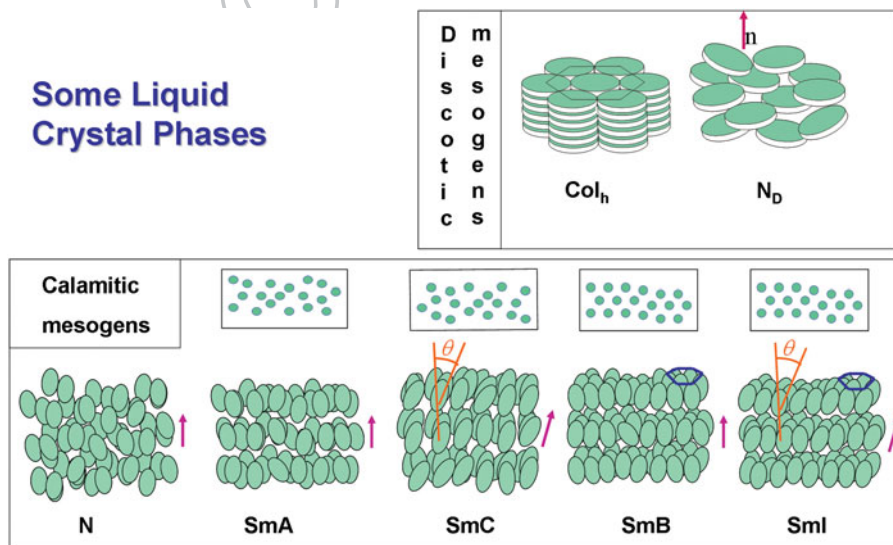

Figure 1. Schematic representation of the most common LC phases. Rectangles above smectic phases show an upper view of the positional distribution of molecules within each layer. The arrow indicates the director (n vector) for N and Sm mesophases.

93   another, in such a way that a preferential direction (the 'director') can be defined, but the
94   positional order is similar to that of a liquid, that is, limited to the first neighbours. In the
95   cases where some positional order is also present in the form of a layered self-organization
96   of the molecules, these mesophases are called smectic. In SmA phases, the long molecular
97   axis of the mesogens is nearly parallel to a director, which in turn is normal to the layers.
98   In SmC phases, the director subtends an angle θ with the normal to the layers. There is no
99   other positional order in SmA and SmC mesophases and each layer behaves as a 2D liquid.
100 Hexatic smectic mesophases exhibit long-range three-dimensional (3D) orientation order
101 and, in addition to the mid-range positional order derived from the layered structure, they
102 also exhibit short-range positional hexagonal order within each layer. That means that a
103 local short-range hexagonal structure is found at a certain position of the layer; moving
104 away 15–60 nm within the same layer, the same kind of hexagonal order will be found, with
105 positions uncorrelated to those of the first region. If the long molecular axes are normal to
106 the layers, the LC phase is called SmB; if the molecules are tilted to the apex or to the sides
107 of the hexagonal mesh, the LC phases are, respectively, called SmI or SmF.

     We shall recall here that the presence of an LC phase, as well as its identification, is
109 usually achieved through the combined use of three different techniques, namely POM, dif-
110 ferential scanning calorimetry (DSC), and variable-temperature powder X-ray diffraction
111 (Tvar-PXRD). POM involves the observation with a transmission microscope (typically,
112 of 200× magnifications) of samples positioned between crossed polarizers and at vary-
113 ing temperatures. The observation of a viscous and birefringent fluid strongly indicates
114 the presence of an LC phase. The nature of the LC phase (N, Sm, Col, etc.) determines the
115 kind of defects it can exhibit. These defects (which extend over distances much longer than
116 those characteristic of defects in crystals) are at the origin of the typical images ('textures')
117 observed for the different LC phases, and often they are diagnostic to identify the kind
118 of LC phase [9]. DSC provides accurate values for the melting and clearing temperatures
119 and associated enthalpy changes (ΔH). Sometimes, ΔH-values assist the assignment of
120 the LC phase (e.g. the enthalpy change expected for an ordered smectic to isotropic liquid
121 (IL) transition is higher than that expected for an N to IL transition). Finally, Tvar-PXRD
122 experiments help to confirm the nature of the different phases exhibited by the studied
123 compound, to validate the transition temperatures detected by POM and DSC, and also to
124 establish the structural parameters characteristic of the LC phase. Indeed, diffraction peaks
125 following a 1:2:3:4 . . . progression in $\sin\theta$-values are characteristic of 1D arrangements
126 typical of smectics; a $1:\sqrt{3}:\sqrt{4}:\sqrt{7}$ . . . progression is characteristic of hexagonal arrays like
127 those found in some columnar LC, and so on. These series of peaks, usually found in the
128 small to mid-θ angles region, afford the assignment of the LC phase and the assessment
129 of its structural parameters, namely inter-lamellar distances for smectics, inter-columnar
130 distances for columnar. The wide-angle scattering region usually conveys additional struc-
131 tural information, like lateral packing in smectics or inter-disc stacking in columnar LC
132 phases, which is often observed as a peak in the 3.5–6 Å range, in addition to a broad halo
133 at ca. 4.5 Å, characteristic of molten aliphatic chains.

134 Actually, crystallographic studies based on XRD might provide detailed information at a
135 molecular level about the way mesogens self-organize themselves in a given mesophase. We
136 will briefly present in what follows four different approaches to the use of XRD studies in
137 the field of Sm LC (columnar mesophases involve their own questions and approaches, and
138 therefore will not be dealt with here). First, we will briefly describe the kind of conclusions

that can be inferred from the simplest Tvar-PXRD experiments. Second, we will review the way XRD studies on mono-domain samples in the Sm phase itself helped to understand the nature of the ordered hexatic phases. Then, we will summarize some interesting examples in which single-crystal (SC) XRD of calamitic mesogens in their solid-state phase provided information about their supra-molecular organization in their LC phases. Finally, we will present a different approach to this issue, namely by combined SCXRD and Tvar-PXRD methods. This approach will be presented through a case study: the structural changes taking place during a crystal-to-SmB transition of a Schiff base (SB) almost deprived of aliphatic chains. In all cases, we will emphasize the molecular aspects of the LC phase organization, and the way crystallography helped to answer specific questions, rather than to analyse in depth the subjacent physics.

2. Powder X-ray diffraction patterns of calamitic mesophases: an overview

PXRD patterns of nematic mesophases usually exhibit a broad peak at small diffraction angles, roughly corresponding to the mean inter-molecular longitudinal distance, and a second broad peak at larger angles corresponding to the mean lateral distance. These peaks, related to the atomic-pair correlation function $g(r)$, are similar to those found for isotropic liquids; their broadness arises from the absence of positional order beyond the first neighbours. For smectics, up to two or three relatively narrow peaks are seen at small to mid-scattering angles for $\sin\theta$-values in the 1:2:3 ratios, while a broader peak is detected at larger angles (typically for $2\theta \approx 20°$ for CuKα). The last peak appears broad for SmA and SmC phases, but much narrower for the hexatic SmB, SmF, and SmI mesophases. The inter-lamellar distance d of Sm mesophases can be inferred from these PXRD patterns, thus affording to model the supra-molecular organization of mesogens. In fact, if d agrees with the molecular length l in a given conformation (e.g. aliphatic chains fully extended), then an SmA phase could be envisaged [14] and this assignment can be confirmed through POM observations. Sometimes $d \cong 2\,l$, in which cases a bi-layer structure (arising, e.g. from head-to-head arrangements of polar mesogens) is suggested [15]. Cases in which $l > d > 2\,l$ have often been interpreted in terms of partly interdigitated bi-layers [16], while the $d < l$ case could correspond to interdigitated layers each one molecule thick [17,18] or, alternatively, to tilted SmC phases [19]. In the last case, POM and/or examination of the chemical structure of the mesogen could assist the assignment. In fact, the corresponding d/l ratio allows one to calculate the tilt angle (θ) of the molecules with respect to the layers through the relation $\cos\theta = d/l$. Typical θ-values lay in the 25–35° range [9]. For mesogens exhibiting multi-block molecular architectures, Sm mesophases have been found as a result of micro-segregation [20] of the 'incompatible' blocks [21] (the term 'incompatible', often misinterpreted, refers to different packing requirements of the molecular blocks, which cannot been simultaneously achieved without micro-segregation).

3. XRD studies on mono-domain samples: assessment on the nature of the ordered smectic mesophases

XRD patterns recorded on oriented samples (achieved by means of applied electric or magnetic fields, surface treatments, etc.) are also useful for assessing the nature of the
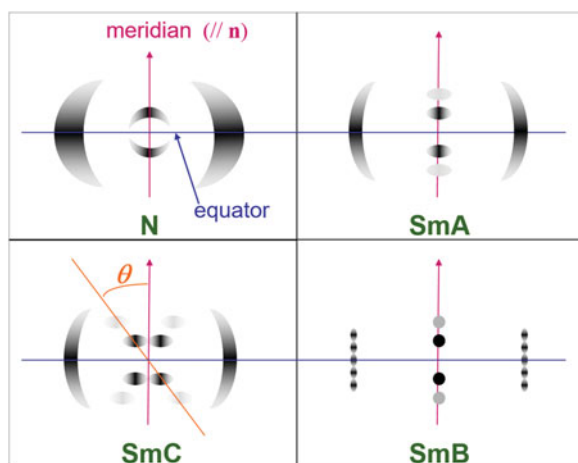
Figure 2. Schematic representation of XRD patterns from aligned samples of different LC phases.

mesophase and to determine some of its structural parameters, beyond the information gathered from un-oriented samples [22]. For nematic mesophases, the diffraction pattern shows two sets of diffuse spots with the shape of broad arcs at mutually perpendicular directions; one set having two symmetrical arcs at low scattering angles and along the meridian (the direction of alignment), the other set consisting in two symmetrical arcs located equatorially and at larger angles, as schematically shown in Figure 2. XRD patterns recorded on oriented samples of smectics usually exhibit one or two pairs of narrow spots on the meridian and a pair of broad arcs at the equator, which become narrower or even split for hexatic mesophases. For tilted Sm mesophases, arcs/spots on the meridian appear as pairs at both θ and $-\theta$ orientations with respect to the meridian.

Donnio and Finkelmann [23] reported an interesting elastomeric material mechanically aligned at the macroscopic scale. Upon mechanical tension, the sample became a quite well-ordered mono-domain, as observed from its 2D XRD pattern; concomitantly, its aspect changed from opaque to transparent.

XRD experiments performed on oriented samples provided valuable structural information to understand the nature of the more ordered Sm phases, a field that has been the subject of active debate [24–32]. Careful crystallographic experiments have been carried out to assess, for example, whether or not a 3D positional order was present in these phases, or the degree of correlation between smectic layers. Very useful information came from XRD experiments on mono-domain samples, obtained by either an applied magnetic field, SC heating, or free-standing films of controlled thickness in the range from 2 to 100 molecular layers. Attention has been paid to the high-angle scattering region of the X-ray diffraction pattern as this provides information about the lateral packing of the molecules within the layers, or positional order between layers. For example, Goodby and co-workers indexed the peaks found in a 2D diffraction pattern obtained from a magnetic field-aligned sample of an SB in its SmB phase under scattering vector $\textbf{\textit{Q}}$ perpendicular to the layers, namely the (100), (101), (102), (103), etc. reflexions of a hexagonal array of laterally and orderly packed molecules [27]. This indexing led them to interpret the spots on the meridian (for $\textbf{\textit{Q}}$ parallel to the layers normal) as the (020) and (040) reflexions and therefore

231   to suggest the presence of a bi-layer structure. Many other X-ray diffraction experiments
232   have been performed on specific mesogens [25–31,33–37]. Based on these studies, some
233   authors suggested that their ordered layered phases exhibited 3D positional order. How-
234   ever, based on different mesogens, other researchers reported that there is no evidence for
235   such positional correlation. This controversy has now been solved. It is currently accepted
236   that some compounds exhibit hexatic smectic mesophases (SmB, SmF, SmI) characterized
237   by long-range orientation bond order (i.e. molecules are essentially parallel to each other
238   not only inside each layer but also from layer to layer) and short-range positional hexag-
239   onal order inside each layer (the layers being essentially uncorrelated from one another)
240   while others exhibit crystalline layered phases like the crystal B, F or E phases (see [38] and
241   references therein).

4. SC crystallography in the mesogen crystalline phase: specific pieces of information about the supra-molecular organization in the Sm mesophase

248   As stated above, SCXRD studies on the crystalline phase of the mesogens can provide
249   additional information about the way these mesophases are organised in the LC state.
250   Interestingly, an early application of this approach was made by Crick in 1953 during
251   his landmark modelling with Watson of the molecular structure of deoxyribonucleic acid
252   (DNA) [39]. From unpublished X-ray diffraction data of Franklin and Gosling on fibres of
253   a sodium salt of nucleic acid from calf thymus (NaDNA), Crick and Watson learned that
254   there was a reversible A-NaDNA $\leftrightarrow$ B-NaDNA transformation upon change of humidity
255   between the lower hydrated crystal A-form (obtained at 75% relative humidity) and the
256   higher hydrated B-form (92% r.h.) [40]. Clearly, these B-NaDNA fibres can now be classed
257   as a lyotropic nematic mesophase consisting in double-stranded DNA fragments oriented
258   parallel to each other and along the fibres but otherwise spatially uncorrelated from each
259   other. The above data also included the monoclinic cell constants and the space group $C2$
260   for the crystal A-form (derived from 2.5 Å resolution data). Crick inferred that the B-form
261   of DNA that he and Watson were modelling should have a molecular structure closely
262   related to the crystal A-NaDNA form. Furthermore, he assumed that the observed crystal-
263   lographic twofold axis symmetry survives the transition to the B-DNA form, that is, this
264   mesogen should show approximate dyadic symmetry. For their double-helical molecular
265   model of B-DNA, this implied that the helices *run in opposite directions* to each other, not
266   a minor constraint in their successful B-DNA modelling efforts. We shall present in the
267   next paragraphs some further representative examples of such an approach in the case of
268   thermo-tropic LC exhibiting Sm mesophases.

269   An interesting example involves a copper-5-alkanoyl-tropolone complex, which shows
270   an SmB phase in the 175–235°C range. Tvar-PXRD results [41] suggested a significant
271   interpenetration of aliphatic chains in this SmB phase, which is strongly supported by the
272   presence of such interdigitation in the crystalline phase [41]. SCXRD studies also helped
273   to understand specific structural features of the SmC mesophase of different compounds.
274   Indeed, Garay et al. found that a biphenyloic acid bearing an oxyethylenic chain exhib-
275   ited an SmC mesophase with $d = 30.8$ Å [42]. The authors calculated l-values of 45.9 and
276   35.2 Å for all-*anti* and some-*gauche* conformations, respectively, and suggested that the

latter should be taken into account giving rise to a tilt angle of 28° rather than the 45° value calculated for the all-*anti* conformation. The structure of the mesogen in its crystalline phase, solved by SCXRD [43], confirmed the suggested *gauche* conformation with an end-to-end length of about 34 Å and also revealed that the tilted lamellar structure is already present in the crystalline phase. In some cases, θ-values calculated for some SmC phases as described above were shorter than the optical tilt angle. Goodby and co-workers [44] ascribed this difference to the cores being more tilted than the aliphatic chains, in agreement with the Wulf steric model for the SmC phase [6]. This suggestion found crystallographic support in, for example, the crystalline structure of an Ni-dithiolate smectogen (see scheme of Figure 3(a)) [45], or those of the *p*-alkoxybenozoic acids [46].

Neve et al. [47] found that Cu(II)-pyridinium salts exhibit Sm mesophases, provided the alkyl chain bears at least 14 methylene units, while shorter chain derivatives are columnar LC, although the crystalline phase of all these compounds already exhibits a lamellar organization. The authors pointed out that this was at odds with the common behaviour of covalent thermo-tropics and suggested that ionic interactions could play an important role for those salts. Bruce et al. [48] found that some alkylsulphate derivatives of silver stilbazole complexes showed N and Sm phases, the first one being unexpected for ionic mesogens. The crystal structure of an octylsulphate (OS) derivative revealed that OS acts as a bridging ligand giving rise to binuclear units whose molecular shape can thus be seen as similar to those of calamitic mesogens with lateral chains, where Sm phases are destabilized in favour of an N phase.

The observed Sm phases became thus unexpected, but again they were explained with the help of SCXRD results. In fact, it turned out that the association of OS to the Ag(I) complex is rather weak, as revealed by the crystallographic O–Ag distances. Binuclear units were also found in the crystal structure of Zn(II) and Pd(II) alkoxydithiobenzoate complexes. Detailed EXAFS studies performed at variable temperature showed that they persist in the N and SmC phases of the Zn(II) complex, but completely disappear in the SmC phase of the Pd(II) analogue [49].

SCXRD studies also provided unexpected results which helped the interpretation of LC structural features. The undulated lamellar mesophase exhibited by some long-chain
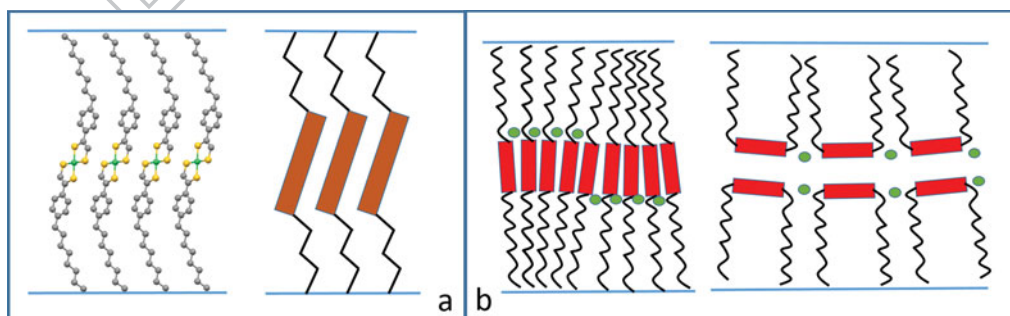
Figure 3. (a) Left: SmC-type layers found in the crystal structure of a Ni-complex [45]. Right: schematic representation of the Wulf's steric model for SmC phase. (b) Left: suggested model for the undulated lamellar phase of Cu(I) aza-macrocyclic complexes under the assumption of a calamitic molecular shape [50]. Right: model suggested for the undulated lamellar phase of analogous Ag(I) complexes, based on the U-shaped molecular structure found in the crystalline phase of the mesogens [51].

macro-cyclic Cu(I) complexes was thought to arise [50] from rod-like mesogens self-organized in undulated mono-layers. An SCXRD study of the crystalline phase of an Ag(I) homologue showed U-shaped molecules that prompted a reinterpretation of the structure as a bi-layer arrangement of folded cations (see scheme of Figure 3(b)) [51].

Finally, another field in which SCXRD provided valuable structural information is that of supra-molecular LC. In fact, SCXRD confirmed the supra-molecular nature of several mesogens, as well as the non-covalent interactions responsible for such assemblies. These interactions range from classical H-bonded carboxylic acids and coordination polymers [52] to engineered supra-molecular entities based on H-bonding [53], π or quadrupolar interactions [54], halogen bonds [55], and combinations of the above [56].

5. An approach combining SCXRD and PXRD: a case study based on an SB

As a contribution of SCXRD to the field of ordered Sm LC, we present here a different approach through a case study, namely the structural changes taking place along the crystal-to-SmB transition of an SB, followed by PXRD in range of temperature, in which SCXRD of the crystalline phase afforded a complete indexation of the PXRD pattern, and showed a pre-organization of the mesogens both in layers and in a pseudo-hexagonal array.

5.1. Structural single crystal X-ray diffraction

The room temperature crystal and molecular structure of the Schiff base 1-(4-((4-dimethylaminobenzylidene)-amino)phenyl) ethanone, hereafter called SB, was reported in [57]. For convenience, we shall summarize here the main results. SB crystallizes in the triclinic $P\bar{1}$ space group with $a = 9.9357(4)$ Å, $b = 17.1016(9)$ Å, $c = 18.1945(9)$ Å, $\alpha = 78.347(4)°$, $\beta = 77.169(4)°$, $\gamma = 76.996(4)°$ and $Z = 8$ molecules per unit cell. There are four independent molecules per asymmetric unit, loosely bond to each other and oriented along the crystal b-axis. These molecules mainly differ from one another in rotations around the σ-bond of the azomethine N-atom with the phenyl ring, hence indicating their conformational degree of freedom.

As shown in the ORTEP [58] plot of Figure 4, besides their mutual interaction through van der Waals forces, the molecules are arranged in a pair of dimers, where they are linked to each other by weak $CH_3 \ldots O$ bonds.

Each set of dimers are arranged in a slightly tilted layered structure parallel to the crystal (010) plane. These layers are partially interdigitated to each other in about half their common width (see Figure 4). At the same time, and through unit cell b-translation, the molecules are arranged into columns along the crystal b-axis. As shown in Figure 5, the columns project onto the crystal a^*c^*-plane as a distorted hexagonal, centred wasp net-like, arrangement.

The above crystallographic results suggest at once that upon increasing temperature, when partial disorder sets in, the system could undergo, by small topological changes, a crystal $\rightarrow$ LC transformation to a smectic phase with a quasi-hexagonal structure. This is sustained by thermal analysis and optical observations. In fact, DSC data show (upon heating) that the SB undergoes two endothermic (first-order) phase transitions, one from 149°C to 153°C ($\Delta H = 3$ kJ mol^{-1}); the other one in the 175–177°C range ($\Delta H = 27$ kJ mol^{-1}). POM observations characterize the first transition as a crystal
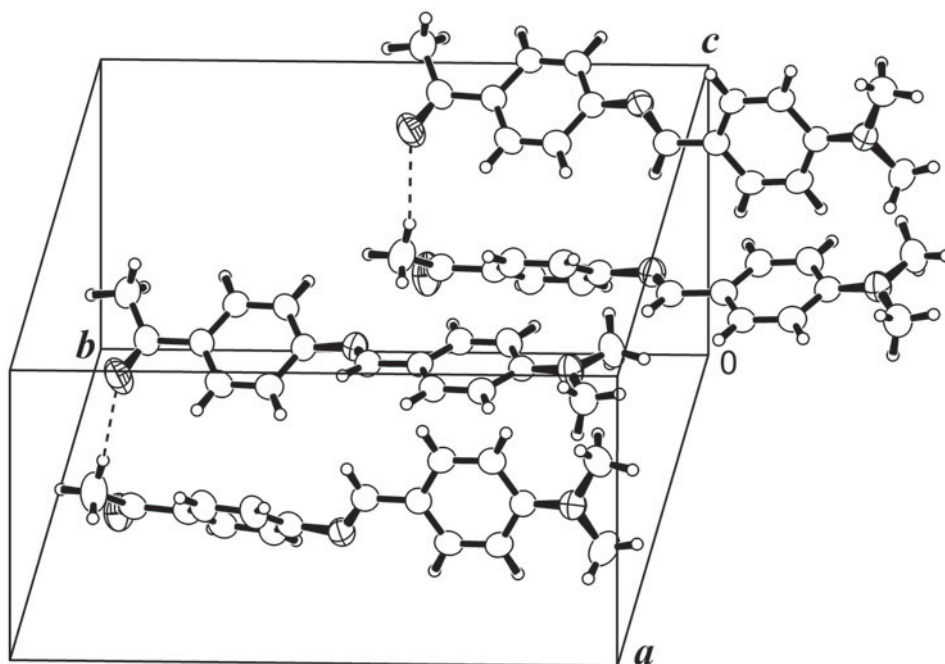
Figure 4. Asymmetric unit content of crystalline SB. Carbon, nitrogen and oxygen atoms are, respectively, denoted by open, crossed and hatched ellipsoids. The molecules are associated in dimeric units and oriented along the crystal b-axis. The dimers are relatively shifted from each other along *b* in about half their length.

(Cr) → hexatic smectic B (LC) phase and the second one as an LC → IL, that is, the phase transformation sequence (RT) Cr → (150°C) LC → (175°C) IL. On cooling, their exothermic phase transitions counterparts are observed at corresponding lower temperatures: 134–131°C ($\Delta H = -27\,\mathrm{kJ\,mol^{-1}}$) and 36–32°C ($\Delta H = -1\,\mathrm{kJ\,mol^{-1}}$), that is, the sequence IL → (133.5°C) LC → (34°C) Cr [57].

5.2. Molecular structure of the SB LC phase by X-ray diffraction

The near close-packed arrangement of molecules embedded in a triclinic lattice described above (see Figure 5) reflects itself (especially at low scattering angle) in an under-laying pseudo-hexagonal symmetry of the X-ray diffraction pattern, an unusual feature to encounter in a general triclinic crystal. In fact, at low resolution, the SB molecules look like featureless rod-like diffracting bodies with a quasi-hexagonal arrangement. This can be clearly appreciated in the weighted reciprocal space of SB shown in Figure 6.

Q2

Figure 6 shows that the relation between the triclinic and pseudo-hexagonal reciprocal unit cell vectors is given in matrix notation by

$$\begin{bmatrix} \underline{a_h}* \\ \underline{b_h}* \\ \underline{c_h}* \end{bmatrix} = \begin{bmatrix} 2 & 0 & 3 \\ 0 & 1 & 0 \\ 0 & 0 & 4 \end{bmatrix} \begin{bmatrix} \underline{a_t}* \\ \underline{b_t}* \\ \underline{c_t}* \end{bmatrix}, \tag{1}$$

where the sub-indexes h and t indicate hexagonal and triclinic lattices.
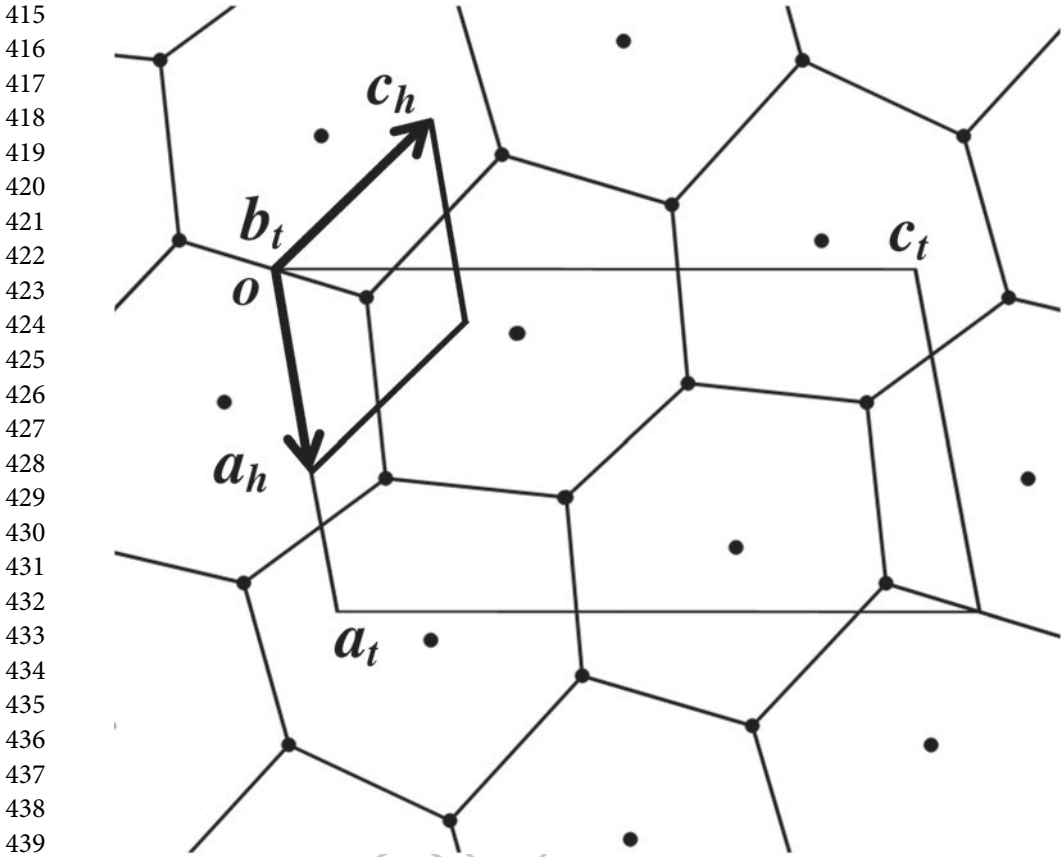
Figure 5. Projection of solid-state SB down the triclinic *b*-axis. The molecules are represented by their centres of mass (filled disks). The figure shows the relation between the triclinic cell (at, ct) and the pseudo-hexagonal cell (ah, ch). The triclinic and quasi-hexagonal *b*-axis are coincident (bt, bh). The hexatic (ah, bh, ch) sub-cell unit volume is 1/8 of the triclinic (at, bt, ct) super-cell unit volume and therefore hosts a single SB molecule.

Let us call $\underset{\sim}{M}$ the 3×3 transformation matrix of Equation (1). Then, the corresponding Miller indices transform (in column matrix notation) according to the inverse transpose matrix $(\underset{\sim}{M}^{-1})^{\mathrm{T}}$, namely

$$\begin{bmatrix} h_h \\ k_h \\ l_h \end{bmatrix} = \begin{bmatrix} 1/2 & 0 & 0 \\ 0 & 1 & 0 \\ -3/8 & 0 & 1/4 \end{bmatrix} \begin{bmatrix} h_t \\ k_t \\ l_t \end{bmatrix}, \tag{2}$$

and therefore, the triclinic $(203)_t$, $(004)_t$ and $(20\bar{1})_t$ reflections become, respectively, the lowest resolution $(100)_h$, $(001)_h$ and $(10\bar{1})_h$ quasi-hexagonal constellation of reflections (see Figure 6).
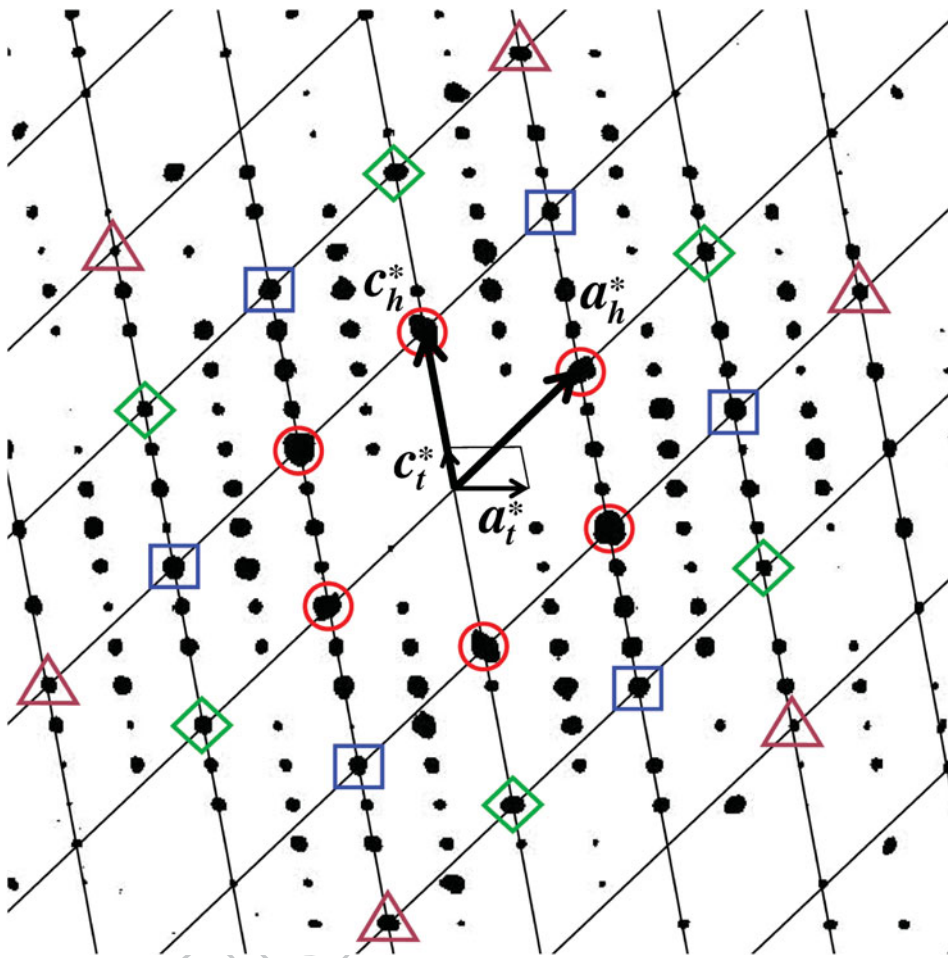
Figure 6. Precession photo-like rendering of single crystal CCD diffractometer data corresponding to *h*0*l* layer of SB showing the relationship between the triclinic and pseudo-hexagonal reciprocal unit cell vectors. For clarity, background scattering has been removed and as a guide to the eyes, the reciprocal *h*0*l* lattice mesh of the quasi-hexagonal SB embedded in the triclinic crystal is included in the figure. Same-shaped geometrical figures encircle quasi D6h symmetry-related reflections. Note that the most intense X-ray diffraction spots in the layer lay on the hexagonal mesh. All reflections, however, are indexed in the triclinic reciprocal lattice.

The corresponding direct triclinic and pseudo-hexagonal unit cell vectors are related by the same $(\underset{\sim}{M}^{-1})^{\mathrm{T}}$ transformation

$$
\begin{bmatrix} \vec{a}_h \\ \vec{b}_h \\ \vec{c}_h \end{bmatrix} = \begin{bmatrix} 1/2 & 0 & 0 \\ 0 & 1 & 0 \\ -3/8 & 0 & 1/4 \end{bmatrix} \begin{bmatrix} \vec{a}_t \\ \vec{b}_t \\ \vec{c}_t \end{bmatrix} \tag{3}
$$

and are graphically indicated in Figure 5.

To further quantify the degree of 'hexagonal' symmetry exhibited by the hexatic recipro-cal lattice super-cell, we selected the sub-set of 'hexagonal' reflections out of the measured

ones for the triclinic lattice, according to the transformations of Equations (1) and (3), employing the program TRANSFORM implemented in the WINGX package [59].

We then calculated the agreement factor among symmetry-related reflections in ranges of resolution with SHELXS of the SHELX suite of programs [60], assuming the Laue D_{6h} group, for both general (hkl) and layer (h0l) reflections. The results are depicted in Figure 7.

Agreement factor in Figure 7 is defined as

$$R_{int} = \sum_{\underline{H}} \sum_{\tilde{R}} |F^2_{\tilde{R}\underline{H}} - F^2_{\underline{H}}(mean)| / \sum_{\underline{H}} \sum_{\tilde{R}} F^2_{\tilde{R}\underline{H}},$$

where $\tilde{R}'s$ are the symmetry operators of point group D_{6h} that generate the 'star' of reciprocal vector $\underline{H}$. The sums include all measured reflections having two or more symmetry equivalents contributing to $F^2_{\underline{H}}(mean)$. From the figure, it can be appreciated the better R_{int} values for (h0l) layer as compared with (hkl) 3D data. This can be mainly traced to the fact that F^2_{h0l} values correspond to the square modulus of the Fourier transform for SB electron density projected along the b-axis and onto the crystal (ac) plane, sampled at the quasi-hexagonal reciprocal lattice points. This projection tends to average out differences in the electron-density distribution along a given molecule and between un-equivalent but closely related SB molecules, hence rendering a higher degree of hexagonal symmetry as compared with 3D data. The systematic improvement of R_{int} observed at low resolution quantifies the above-mentioned statement that in this limit the X-rays see undistinguished and featureless rod-like diffracting objects with a near close-packing arrangement.
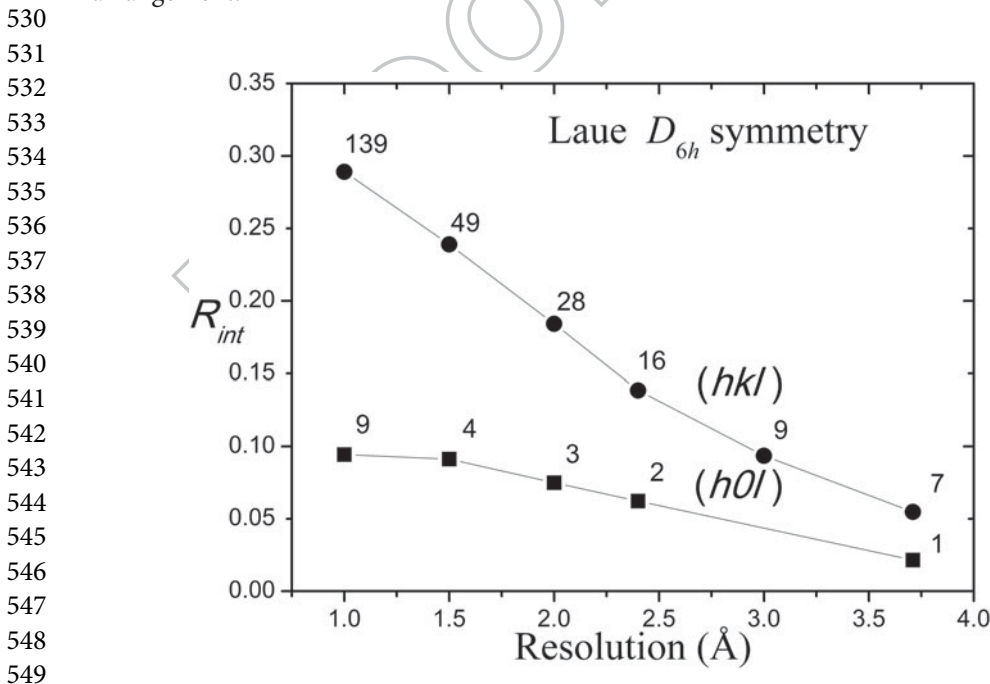
Figure 7. Agreement Rint factor among Laue D6 h symmetry-related reflections embedded in the room temperature weighted SB reciprocal triclinic lattice. The integers on the Rint values are the number of quasi-hexagonal unique reflections measured within the indicated resolution limits.

5.3. Powder X-ray diffraction vs. temperature

We shall now examine structurally the phase transformation sequence (RT) Cr → (150°C) LC → (175°C) IL by PXRD vs. temperature measurements. In Figure 8, it is compared the observed RT (20°C) PXRD pattern of SB with the calculated one [61] from single crystal X-ray diffraction data [57] and also with the diffraction data just below the (RT) Cr → (150°C) LC transition (at 140°C) and just above the transformation to the mesogenic phase (at 160°C). An X-ray diffractogram run at 175°C showed the featureless pattern expected for an IL.

As expected for molecular solids, the SB crystal diffracted poorly. In fact, the intensity of only about a 64% of the SC reflections measured up to 0.82 Å resolution was above two times the experimental standard errors. Despite the few lines observed in the PXRD pattern, however, the diffractograms include valuable diagnostic lines that, by comparison with the SC data, afford definite conclusions above the structure of the smectic phase. For convenience, we shall group these lines into three sets, namely, (i) the quasi-hexagonal diffraction lines, (ii) the interdigitated layer lines and (iii) the triclinic reflections.

(i) Concerning the first set, the 20°C PXRD pattern shows a diffraction peak at $2\theta = 20.10°$ which is the strongest one within a set of three reflections and
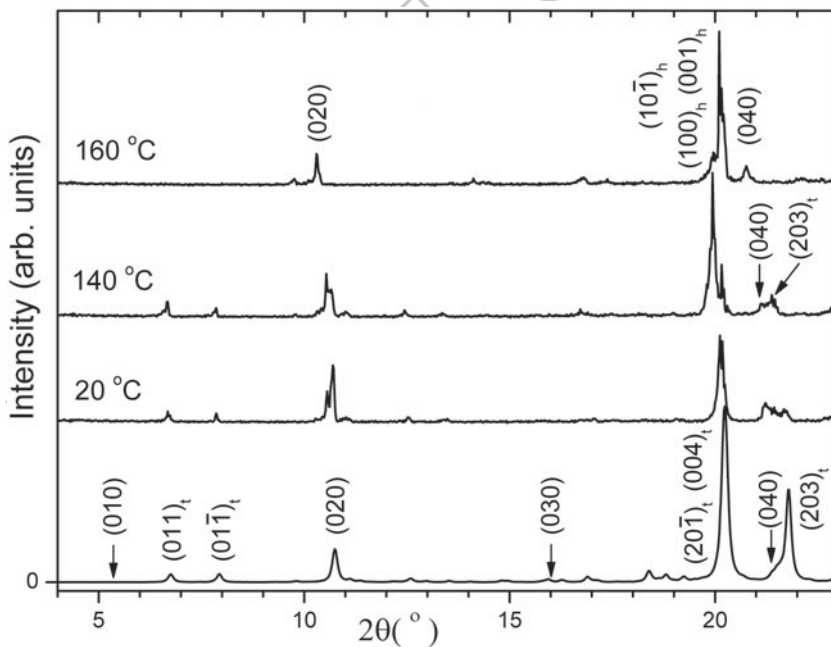

Figure 8. Lower trace: powder X-ray diffraction (PXRD) pattern calculated from the solid-state molecular structure of SB determined at room temperature by single crystal X-ray diffraction methods. Upper traces: experimental PXRD pattern vs. temperature collected with CuKα radiation. Subscripts 't' and 'h' indicate Bragg reflections, respectively, indexed in the triclinic lattice and the quasi-hexagonal sub-lattice. Unsubscripted (0k0) reflections are the signature of layered structure common to both lattices. The 2θ angles where the systematically weak low-resolution (0k0) reflections with k odd should appear are indicated by vertical arrows. Note the vanishing of triclinic and lines upon the transformation to the hexatic CL phase.

corresponds to the (unresolved) superposition of $(20\bar{1})_t$ and $(004)_t$ triclinic diffractions. The other line in the set shows up at $2\theta = 21.72°$ and corresponds to $(203)_t$ reflection. As shown by Equation (2), these three triclinic diffraction lines transform into the $(10\bar{1})_h$, $(001)_h$ and $(100)_h$ hexagonal lines. These integrate (upon the inclusion of their Friedel counterparts) the lowest resolution quasi-hexagonal constellation of reflections (see Figure 6) which originates in the near close-packing of SB molecules oriented along the triclinic b-axis. Upon heating the crystal to 140°C, it is appreciated from the diffraction pattern that SB basically maintains its 20°C triclinic structure with the $(203)_t$ reflection almost merged with the (040) reflection because anisotropic crystal behaviour where the thermal dilatation constant perpendicular to the b-axis ($\alpha_\perp = 5.8 \times 10^{-5°}C^{-1}$) is twice as much as the one along this axis ($\alpha_\parallel = 2.6 \times 10^{-5°}C^{-1}$). On further heating to 160°C, it is observed that there is the near collapse of all three lines upon the transition to the crystal liquid phase, hence indicating a smectic hexagonal arrangement. This can be interpreted as the thermo-tropic transformation from the distorted hexagonal, wasp net-like, arrangement observed in the triclinic crystal to the more closely hexagonal, bee net-like lattice, of the LC phase when thermal rotational disorder of the molecules around the b-axis sets in. From the overlapping feature at $2\theta = 20.12°$ in the 160°C PXRD pattern, it can be calculated the hexagonal cell constant $a = c = 5.1\,Å$ of the mesogenic state which is equal to the distance between neighbouring molecular columns, a value close to (and slightly larger than) the lateral inter-molecular average distance observed in the 20°C crystal.

(ii) The other set of reflections refers to the long-range order along the b-axis. The diffraction lines observed at 2θ-values of 10.70° and 21.20° in the 20°C PXRD pattern correspond, respectively, to the (020) and (040) reflections and they are a signature of the interdigitation of layers observed in the crystal. As mentioned above, the intercalation is about one half of the molecular length, that is, nearly half the dimension of the b-axis, a fact that explains the relatively high intensity of (020) reflection and also the observed systematically very weak low-resolution $(0k0)$ reflections with k odd. The diffractograms of Figure 8 clearly show that these diagnostic lines, and therefore the interdigitated layered structure, survive both crystal heating and the transition to the LC phase.

(iii) Finally, the vanishing of the low-resolution triclinic $(011)_t$ and $(01\bar{1})_t$ lines upon the Cr → LC transformation could be interpreted as further proof of a structurally more symmetric LC mesophase as compared with the crystal phase.

6. Conclusions

(1) Despite the many useful techniques employed to probe the physical properties of thermo-tropic smectic LC phase, no single method can provide the wealth of structural information at the molecular level afforded by X-ray diffraction, especially when the structure of the compound in its crystal phase is available.

(2) Different approaches based on XRD experiments could be followed, depending on the specific structural questions about the structure of the Sm phase under study: Tvar-PXRD, XRD on mono-domain samples in the Sm phase, SCXRD of the mesogen in its crystalline phase, or a combination of SCXRD and PXRD.

(3) Combined single crystal and variable-temperature powder X-ray diffraction provides a powerful tool to infer a detailed molecular structure for smectic thermo-tropic phases.

(4) Following this last approach, we described a case study as an illustration that established that upon heating, SB undergoes a crystal to LC phase transition (at about 150°C) to a smectic SmB hexagonal slightly (if at all) tilted and interdigitated phase which closely resembles topologically its room temperature triclinic crystal.

(5) The structural results predict for the SB LC phase an optically uniaxial positive behaviour. Based on the PXRD vs. temperature data, it is estimated that there is a perpendicular-to-molecular long axis dilation coefficient roughly twice as large as the longitudinal one, a fact that suggests that the onset of the crystal → LC transition is promoted by the set in of thermal rotational disorder of the molecules around their long axes. The distance between side neighbouring molecular columns in the CL hexagonal arrangement is of about 5.1 Å, close to (and slightly larger than) the average inter-molecular distance observed in the room temperature crystal.

Acknowledgements

Disclosure statement

No potential conflict of interest was reported by the authors.   Q3

Funding

Notes on contributors

Oscar Enrique Piro received his Doctorate in Physics (PhD) from the National University of La Plata (UNLP), Argentina, in 1977, in the field of Solid State Physics. He made post-doctoral research at the Department of Biophysics and Theoretical Biology of the University of Chicago, working on X-ray crystallography of biological macromolecules (1978–1980). He is one of the pioneers in the information theoretical approach (maximum entropy) to the solution of the 'phase problem'. Upon his return to Argentina, he became a Research Fellow of CONICET and currently he is Full Professor of UNLP. His research interest is grounded in Solid State Physics, particularly in Structural Crystallography by X-ray diffraction methods and also in the optical and spectroscopic (mainly infra-red and Raman) properties of crystals. Currently, he works on the structure–physicochemical properties relationship of inorganic, organic, metal-organic (including minerals), bioorganic and bioinorganic, pharmaceutical (both natural and synthetic) and supra-molecular materials.

Gustavo Alberto Echeverría received his Doctorate in Physics (PhD) in 1997 from the National University of La Plata (UNLP), Argentina. During his PhD, he got a fellowship from the Japan International Cooperation Agency (JICA) to spend 6 months doing research at Catalysis Research Center, Hokkaido University, Sapporo, Japan. At present, he is Research Fellow of CONICET and Professor of UNLP. His research interests are in condensed matter physics, mainly in Structural Crystallography by X-ray diffraction methods to study the structure–property relationship of functional materials of biological and environmental impact.

Fabio Daniel Cukiernik studied Chemistry at the University of Buenos Aires, Argentina (1983–1989), then obtained the DEA en Chimie Moléculaire (1990) and PhD (1993) degrees from the Université Scientifique, Technique et Médicale Joseph Fourier (Grenoble I), France. He was one of the founders of the Chemistry section at UNGS, and is currently Research Fellow of Conicet and Associate Professor at the Department of Inorganic, Analytical and Physical Chemistry of the School of Natural and Exact Sciences of the University of Buenos Aires, where he is the head of the Liquid Crystals research group. His research interests involve the design, synthesis and characterization of liquid crystalline materials, as well as the study of their supra-molecular organization and magnetic properties. His research is focused mainly on coordination polymers and main-chain triphenylene-containing covalent polymers; the way non-covalent interactions contribute to their self-organization is a permanent query. X-ray diffraction techniques (both SC and powder), local spectroscopic probes and computational simulations (QM, MM and DM) are among the techniques he mostly uses to provide answers to these questions.

References

[1] Lehmann O. Über fliessende Kristalle. Z Phys Chem. 1889;4:462–472.

[2] De Gennes PG. Some remarks on the polymorphism of smectics. Mol Cryst Liq Cryst. 1973;21:49–76.

[3] Osipov MA. Molecular theories of liquid crystals. Section 2, Chapter III, Volume 1. In: Demus D, Goodby J, Gray GW, Spiess HW, Vill V, editors. Handbook of liquid crystals. Weinheim: Wiley-VCH; 1998. p. 40–71.

[4] Mc Millan WL. Simple molecular theory of the smectic-C phase. Phys Rev A. 1973;8:1921–1929.

[5] Wulf A. Steric model for the smectic-C phase. Phys Rev A. 1975;11:365–375.

[6] Cotter MA. Molecular theories of nematic liquid crystals. Mol Cryst Liq Cryst. 1983;97:29–47.

[7] De Gennes PG, Prost J. The physics of liquid crystals. Oxford: Oxford University Press; 1993.

[8] Velasco E, Mederos L, Sluckin TJ. Molecular theory of smectic liquid crystals. Liq Cryst. 1996;20:399–409.

[9] Dierking I. Textures of liquid crystals. Weinheim: Wiley-VCH; 2001.

[10] Kwok HS, Naemura S, Ong HL, editors. Progress in liquid crystal science and technology. Singapore: World Scientific; 2013.

[11] Baron M. Definitions of basic terms relating to low-molar-mass and polymer liquid crystals. Pure Appl Chem. 2001;73:845–895.

[12] Reinitzer F. Beiträge zum Kenntniss des Cholesterins. Monatsh Chem. 1888;9:421–441.

[13] Demus D. Chemical structure and mesogenic properties. Chapter VI, Volume I. In: Demus D, Goodby J, Gray GW, Spiess HW, Vill V, editors. Handbook of liquid crystals. Weinheim: Wiley-VCH; 1998. p. 133–187.

[14] Diele S, Manke S, Weissflog W, et al. Smectic a phases with strings of interdigitated molecules in swallow tailed compounds. Liq Cryst. 1989;4:301–307.

[15] Hardouin F, Levelut AM, Benattar JJ, et al. X-rays investigations of the smectic A1–smectic A2 transition. Solid State Commun 1980;33:337–340.

[16] Chen J, Bai X, Jing S, et al. Self-assembly of imidazolium-based rodlike ionic liquid crystals: transition from lamellar to micellar organization. Chem Eur J. 2010;16:4588–4601.

[17] Pal SK, Raghunathan VA, Kumar S. Phase transitions in novel disulphide-bridged alkoxy-cyanobiphenyl dimers. Liq Crystallogr. 2007;34:135–141.

[18] Andreu R, Barberá J, Garín J, et al. Synthesis and liquid crystal behaviour of tetrathiofulvalenes containing cyanobiphenyloxy groups. J Mater Chem. 1998;8:881–887.

[19] Rampon DS, Rodembusch FS, Scneider JMFM, et al. Novel selenoesters fluorescent liquid crystalline exhibiting a rich phase polymorphism. J Mater Chem. 2010;20:715–722.

[20] Tschierske C. Non-conventional liquid crystals – the importance of micro-segregation for self-organization. J Mater Chem. 1998;8:1485–1508.

[21] Ungar G, Noble K, Percec V, et al. X-ray diffraction study of polyphilic smectic liquid crystals. J Mater Sci. 2000;35:5241–5246.

[22] Hiraoka K, Uematsu Y, Stein P, et al. X-Ray diffraction studies on the phase-transformational behavior of a smectic liquid-crystalline elastomer composed of chiral mesogens. Macromol Chem Phys. 2002;203:2205–2210.

[23] Donnio B, Wermter H, Finkelmann H. A simple and versatile synthetic route for the preparation of main-chain, liquid-crystalline elastomers. Macromolecules 2000;33:7724–7729.

[24] De Gennes PG, Sarma G. Tentative model for the smectic-B phase. Phys Lett. 1972;38: 219–220.

[25] De Jeu WH, De Poorter JA. X-ray diffraction of the smectic phases of N-(p-n-heptyloxybenzylidene)-$p\hat{E}\acute{z}$-n-pentylanyline. Phys Lett. 1977;61:114–116.

[26] Moncton DE, Pindak R. Long-range order in two- and three-dimensional smectic-B liquid crystal films. Phys Rev Lett. 1979;43:701–704.

[27] Leadbetter AJ, Mazid MA, Kelly BA, et al. Structure of the smectic-B phase and the nature of the smectic-B to smectic-H transition in the N-(4-n-alkoxybenzylidene)-4′-alkylanilines. Phys Rev Lett. 1979;43:630–633.

[28] Benattar JJ, Doucet J, Lambert M, et al. Nature of the smectic-F phase. Phys Rev A. 1979;20:2505–2509.

[29] Pindak R, Moncton DE, Davey SC, et al. X-ray observation of a stacked hexatic liquid-crystal-B phase. Phys Rev Lett. 1981;46:1135–1138.

[30] Bruinsma R, Aeppi G. Hexatic order and herring-bone packing in liquid crystals. Phys Rev Lett. 1982;48:1625–1628.

[31] Górecka E, Chen L, Pyzuk W, et al. X-ray studies of the hexatic phase in liquid crystals with a crystal-B–hexatic-B–smectic-A phase sequence. Phys Rev A. 1994;E50:2863–2867.

[32] De Gaetani L, Tani A. Sixfold bond orientational properties of a model liquid crystal in the dimensional crossover of B phases: a computer simulation study. J Chem Phys. 2007;126:064909(1-5).

[33] Albertini G, Fanelli E, Melone S, et al. Evidence by X-ray diffraction for hexatic B and crystal B structures in a pure compound. Solid State Commun. 1984;49:1143–1146.

[34] Davey SC, Budai J, Goodby JW, et al. X-ray study of the hexatic-B-to-smectic-A phase transition in liquid crystal films. Phys Rev Lett. 1984;53:2129–2132.

[35] Sirota EB, Pershan PS, Sorensen LB, et al. X-ray studies of tilted hexatic phases in thin liquid-crystal films. Phys Rev Lett. 1985;55:2039–2042.

[36] Collett J, Sorensen LB, Pershan PS, et al. X-ray scattering study of restacking transitions in the crystalline-B phases of heptyloxybenzylidene heptylanyline. Phys Rev A. 1985;32:1036–1043.

[37] Lobo CV, Prasad SK, Rao DSS. X-ray and dielectric measurements of the smectic A–hexatic-B transition in bulk and confined geometries. Phys Rev. 2004;E69:051706(1-8).

[38] Pershan PS. Scattering from mesomorphic structures. Volume B, Chapter 4.4. In: Shmueli U, editor. International tables for crystallography. London: Kluwer; 2006. p. 449–465.

[39] Watson JD, Crick FHC. A structure for deoxyribose nucleic acid. Nature. 1953;171: 737–738.

[40] Franklin RE, Gosling RG. The structure of sodium thymonucleate fibres. II. The cylindrically symmetrical Patterson function. Acta Crystallogr. 1953;6:678–685.

[41] Elliott JM, Chipperfield JR, Clark S, et al. Criteria for liquid crystal formation in 5-alkoxy-, 5-alkylamino, and 5-alkanoyl-tropolone complexes of transition metals (CuII, ZnII, NiII, CoII, UO2VI, VOIV). The first uranium metallomesogen. Crystal structure of bis(5-hexadecyloxytropolonato)copper(II). Inorg Chem. 2002;41:293–299.

[42] Montani RS, Hegguilustoy CM, Del Rosso PG, et al. 4′-(2-(2-Ethoxyethoxy)ethoxy)biphenyl-4-carboxylic acid-a polar smectogen for amphipathic liquid crystals. Tetrahedron Lett. 2009;50:5231–5234.

[43] Montani RS, Garay RO, Cukiernik FD, et al. 4′-[2-(2-Ethoxyethoxy)ethoxy]biphenyl-4-carboxylic acid: correlation between its crystalline and smectic phases. Acta Crystallogr. 2009;C65:o81–o84.

[44] Mills JT, Gleeson HF, Goodby JW, et al. X-ray and optical studies of the tilted phases of materials exhibiting antiferroelectric, ferrielectric and ferroelectric mesophases. J Mater Chem. 1998;8:2385–2390.

[45] Cotrait M, Gaultier J, Polycarpe C, et al. Structure d'un complèxe de métal de transition smectique: Le Bis{[(octy-4phényl)-1-éthylènedithiolato-1,2](2-)-S,S′}nickel, $C_{32}H_{44}NiS_4$. Acta Crystallogr. 1983;C39:833–835.

[46] Kuz'mina LG, Kucherepa NS, Pestov SM, et al. Molecular and crystal structure of 4-alkoxybenzoic acids: design of the mesogenic phase. Crystallogr Rep. 2009;54(5):862–879.

[47] Neve F, Francescangeli O, Crispini A, et al. A2[MX4] copper(II) pyridinium salts. From ionic liquids to layered solids to liquid crystals. Chem Mater. 2001;13:2032–2041.

[48] Adams H, Bailey NA, Bruce DW, et al. Mesomorphic stilbazole complexes of silver octyl sulfate. J Mater Chem. 1992;2:395–400.

[49] Guillon D, Bruce DW, Maldivi P, et al. EXAFS studies of some alkoxydithiobenzoate complexes of Zn(II) and Pd(II) in their liquid-crystal phases. Chem Mater. 1994;6:182–189.

[50] Neve F, Ghedini M, Levelut AM, et al. Ionic metallomesogens. Lamellar mesophases in Cu(I) azamacrocyclic complexes. Chem Mater. 1994;6:70–76.

[51] Neve F, Ghedini M, De Munno G, et al. Ionic amphiphilic metallomesogens. Chem Mater. 1995;7:688–693.

[52] Serrette A, Carroll PJ, Swager TM. Tunning the intermolecular dative interaction in vanadium-oxo linear chain compounds: formation of a new type of liquid crystalline polymers. J Am Chem Soc. 1992;114:1887–1889.

[53] Willis K, Price DJ, Adams H, et al. Hydrogen-bonded liquid crystals from alkoxystilbazoles and 3-cyanophenols: structural control of mesomorphism. Molecular structure of the complex between 4-cyanophenol and 4-octyloxystilbazole. J Mater Chem. 1995;5:2195–2199.

[54] Bruce DW. Liquid crystals formed from specific intermolecular interactions. Volume 7, Gale PA, Steed JW, editors. Supramolecular chemistry: from molecules to nanomaterials. Wiley; 2012. p. 3493–3514.

[55] Nguyen HL, Horton PN, Hursthouse MB, et al. Halogen bonding: a new interaction for liquid crystal formation. J Am Chem Soc. 2004;126:16–17.

[56] Cho CM, Wang X, Li JJ, et al. Synthesis and self-assembly of halogen-bond donor-spacer-hydrogen-bond donor molecules: polymeric liquid crystals induced by combination of intermolecular halogen and hydrogen-bonding interactions. Liq Crystallogr. 2013;40:185–196.

[57] Rocha M, Di Santo A, Echeverria GA, et al. Supramolecular self-assembly of a new multi-conformational Schiff base through hydrogen bonds: crystal structure, spectroscopic and theoretical investigation. J Mol Struct. 2017;1133:24–36.

[58] Farrugia LJ. ORTEP-3 for windows – a version of ORTEP-III with a graphical user interface (GUI). J Appl Crystallogr. 1997;30:565–565.

[59] Farrugia LJ. WinGX suite for small-molecule single-crystal crystallography. Appl Crystallogr. 1999;32:837–838.

[60] Sheldrick GM. A short history of SHELX. Acta Crystallogr. 2008;64:112–122.

[61] Yvon K, Jeitschko W, Parthe E. LAZY PULVERIX – a computer program for calculating theoretical X-ray and neutron diffraction powder patterns. J Appl Crystallogr. 1977;10:73–74.

Appendix

Temperature-dependent polycrystalline and crystal liquid XRD data for the case study described in Section 6 were obtained with a PANalytical X'Pert PRO diffractometer, using CuKα radiation ($\lambda = 1.5406$ Å) from an X-ray tube operated at 40 kV and 40 mA. The X-ray diffraction pattern was collected in the $4° \leq 2\theta \leq 34°$ range, with 0.02° step width and 1 s counting time per step employing the Bragg-Brentano θ-θ geometry, a scintillation counter and an exit beam graphite monochromator. Estimated error in measured 2θ-values is 0.03°. The sample holder was heated with a resistor and the temperature controlled with an Anton Paar, model TTK2-HC, device fitted with a Pt-100 class-A temperature sensor working at 0.1 K resolution. Because of unavoidable temperature gradient at the sample holder, the absolute sample temperatures are only known to within 1 K.